

Two Novel Metal-Organic Frameworks Based on Pyridyl-Imidazole-Carboxyl Multifunctional Ligand: Selective CO₂ Capture and Multiresponsive Luminescence Sensor

Dou-Dou Feng ^a, Yu-Di Zhao^a, Xiao-Qing Wang^{*a}, Dong-Dong Fang^a, Jing Tang^a, Li-Ming Fan^a and Jie Yang ^{*b}

a. North University of China, Tai Yuan, P. R. China. E-mail; xqwang@nuc.edu.cn;

b. Liaocheng University, Liaocheng, P. R. China. E-mail; yangjie_lcu@126.com

The single-site Langmuir-Freundlich model for CO₂ and CH₄ adsorption isotherms

In order to compare the efficiency of complex **1** for CO₂/CH₄ and CO₂/N₂ separation, we used the IAST of Myers and Prausnitz along with the pure component isotherm fits to determine the molar loadings in the mixture for specified partial pressures in the bulk gas phase. The measured experimental data on pure component isotherms for CO₂ and CH₄, in terms of excess loadings, were first converted to absolute loading using the Peng-Robinson equation of state for estimation of the fluid densities. The absolute component loadings at 273 K were fitted with a single-site Langmuir-Freundlich model (Equation 1).

$$N = a \times \frac{bp^c}{1 + bp^c} \quad (1)$$

Here, a is saturation capacity and b and c are constant. The fitting parameters of equation 1 as well as the correlation coefficients (R²) are listed in Table S2.

Table S1 Selected bond lengths (Å) and angles (°) for complexes **1** -**2**.

Mn1—O2 ⁱ	2.163 (5)	Mn1—O1	2.187 (5)
Mn1—O2 ⁱⁱ	2.163 (5)	Mn1—N1 ^{iv}	2.217 (6)
Mn1—O1 ⁱⁱⁱ	2.187 (5)	Mn1—N1 ^v	2.217 (6)
O2—Mn1 ^{vi}	2.163 (5)	N1—Mn1 ^{vii}	2.217 (6)

C7—C10	1.485 (10)	C10—C11	1.375 (10)
C7—C8	1.382 (10)	C5—C4	1.352 (10)
C7—C6	1.365 (11)	C5—C6	1.371 (11)
O2 ⁱⁱ —Mn1—O2 ⁱ	180.0 (3)	O2 ⁱⁱ —Mn1—O1	93.0 (2)
O2 ⁱⁱ —Mn1—O1 ⁱⁱⁱ	87.0 (2)	O2 ⁱ —Mn1—O1 ⁱⁱⁱ	93.0 (2)
O2 ⁱ —Mn1—O1	87.0 (2)	O2 ⁱⁱ —Mn1—N1 ^v	95.2 (2)
O2 ⁱ —Mn1—N1 ^{iv}	95.2 (2)	O1 ⁱⁱⁱ —Mn1—O1	180.0
O2 ⁱ —Mn1—N1 ^v	84.8 (2)	O1 ⁱⁱⁱ —Mn1—N1 ^v	90.5 (2)
O2 ⁱⁱ —Mn1—N1 ^{iv}	84.8 (2)	O1—Mn1—N1 ^v	89.5 (2)
O1 ⁱⁱⁱ —Mn1—N1 ^{iv}	89.5 (2)	N1 ^v —Mn1—N1 ^{iv}	180.0 (3)
O1—Mn1—N1 ^{iv}	90.5 (2)	C1—N1—Mn1 ^{vii}	130.0 (5)

Symmetry codes: (i) $x-1, y, z$; (ii) $-x+1, -y, -z$; (iii) $-x, -y, -z$; (iv) $-x-1, y-1/2, -z+1/2$; (v) $x+1, -y+1/2, z-1/2$; (vi) $x+1, y, z$; (vii) $-x-1, y+1/2, -z+1/2$.

Ag1—O1 ⁱ	2.337 (3)	N1—C1	1.369 (5)
Ag1—N1	2.179 (3)	C24—C12	1.485 (5)
Ag1—N5 ⁱⁱ	2.179 (3)	C24—C25	1.387 (5)
N3—C14	1.343 (5)	C24—C29	1.389 (5)
N3—C10	1.345 (4)	N5—C22	1.369 (5)
C18—C17	1.381 (5)	C11—C12	1.379 (5)
C18—C19	1.373 (5)	C11—C10	1.392 (5)
N4—C23	1.352 (4)	C13—C14	1.386 (5)
N4—C21	1.369 (5)	C13—C12	1.394 (5)
N1—Ag1—O1 ⁱ	111.95 (11)	C12—C11—C10	120.6 (4)
N1—Ag1—N5 ⁱⁱ	138.58 (13)	C10—C11—H11	119.7
N5 ⁱⁱ —Ag1—O1 ⁱ	109.06 (12)	C27—C26—H26	119.5
C30—O1—Ag1 ⁱⁱⁱ	116.7 (3)	C19—C18—C17	119.6 (4)
C17—C18—N4	120.1 (4)	C26—C27—C30	121.4 (4)

C19—C18—N4	120.3 (3)	C28—C27—C30	120.6 (4)
Symmetry codes: (i) $-x+1, y+3/2, -z+1/2$; (ii) $-x+2, -y+1, -z$; (iii) $-x+1, y-3/2, -z+1/2$.			

Table S2 Equation parameters for the single-site Langmuir-Freundlich model.

Adsorbates	a (mmol/g)	b (kPa ⁻¹)	c	R ²
CO ₂	4.11	0.0422	0.728	0.99921
N ₂	0.838	0.00228	1.04	0.9994
CH ₄	2.15	0.00902	0.973	0.99994

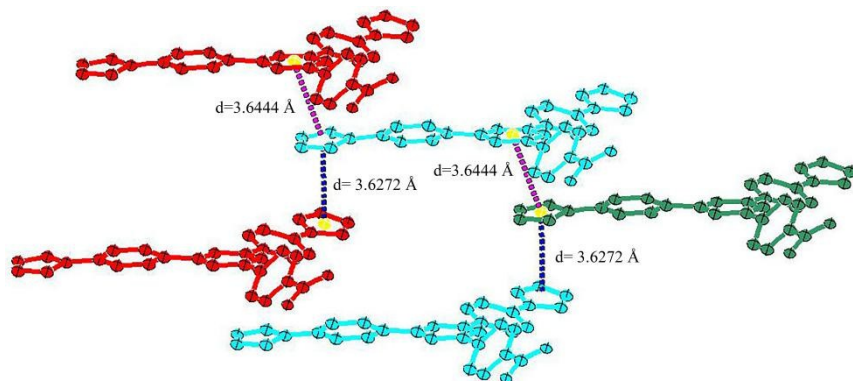


Fig .S1 The π -stacking interaction of complex **2**.

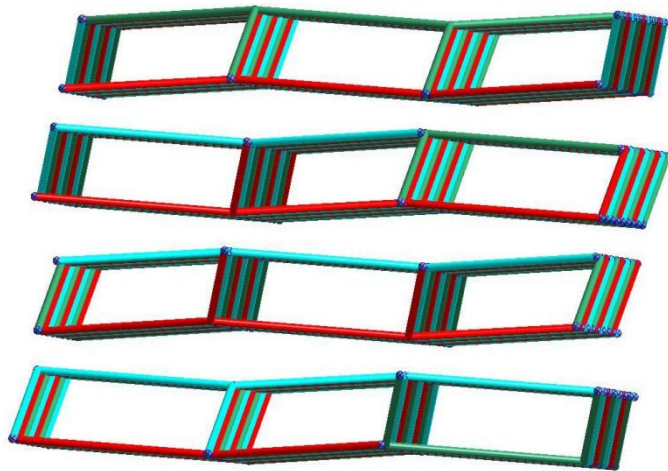


Fig .S2 The 3D supramolecular structure of complex 2.

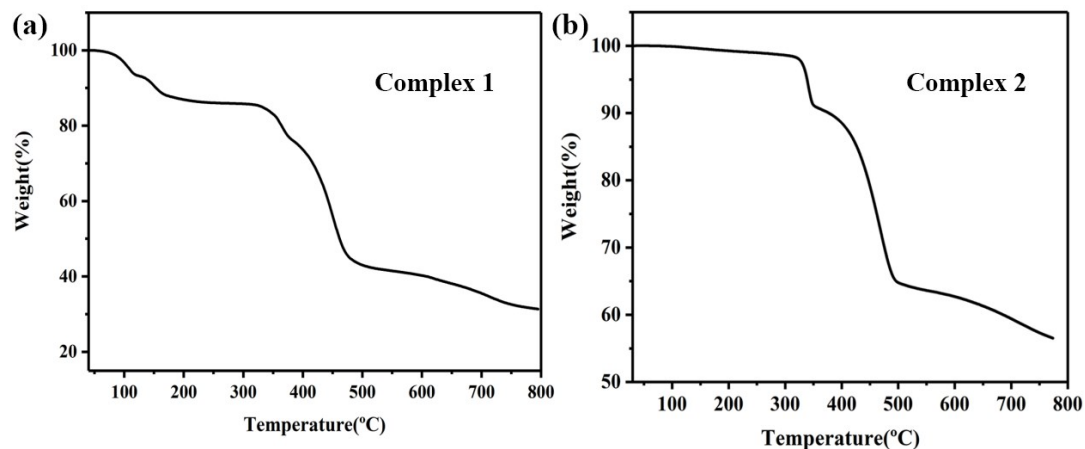


Fig .S3 (a) The TGA curve of complex 1; **(b)** The TGA curve of complex 2.

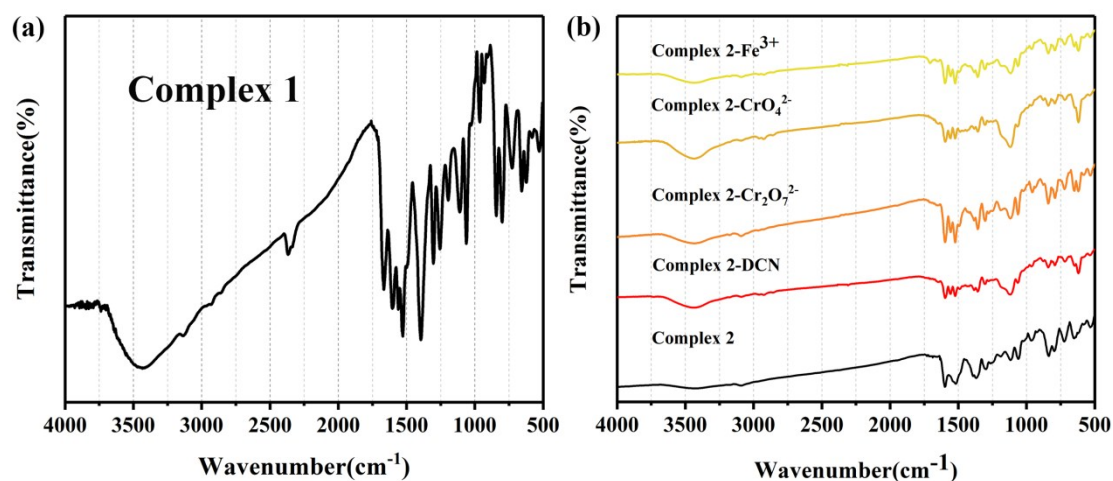


Fig .S4 (a) The IR of complex 1; **(b)** The IR of complex 2 before and after exposure to different

analytes.

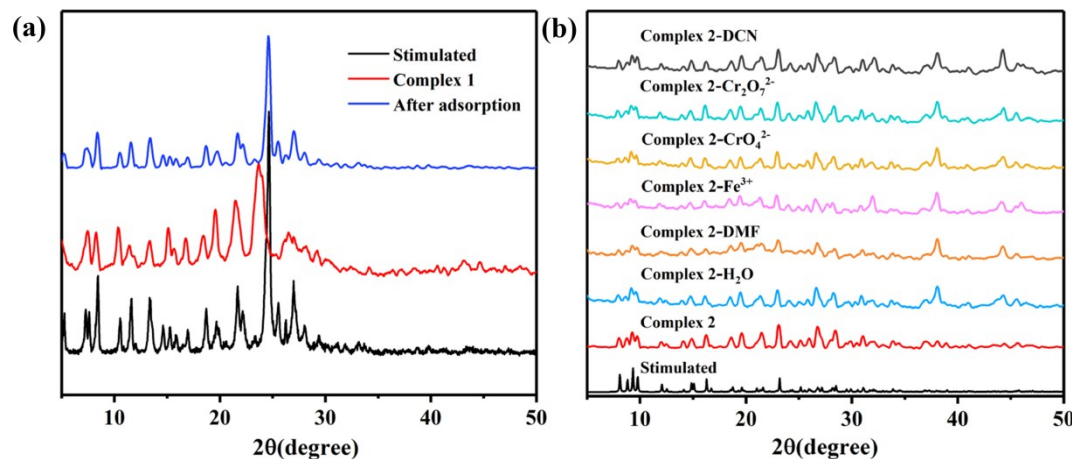


Fig .S5 (a)The PXRD patterns of complex **1**, stimulated and **1a** (after adsorption); (b)The PXRD patterns of complex **2** before and after exposure to different analytes.

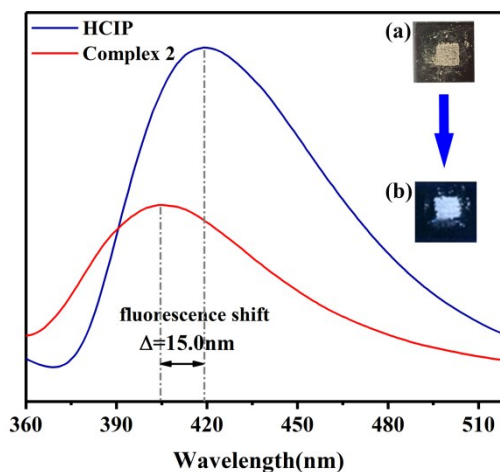


Fig .S6 Photoluminescent emission spectrum of HCIP and **2** in the solid state with the excitation at 280 nm at room temperature. Insets show digital photograph of **2** in daylight (**a**) and 365 nm UV light (**b**).

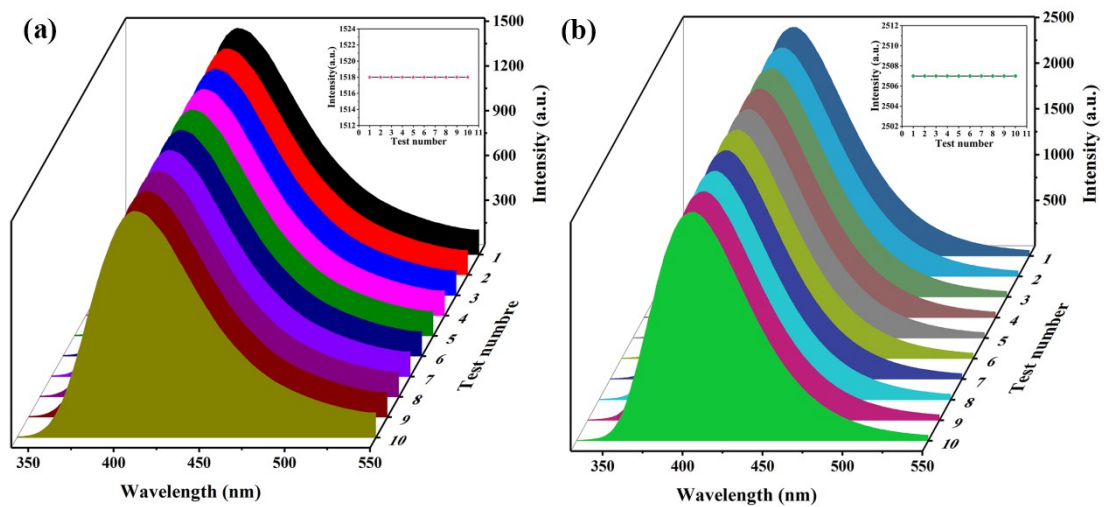


Fig. S7 **(a)** The fluorescence intensity of **2** was measured 10 times in water; **(b)** The fluorescence intensity of **2** was measured 10 times in DMF.

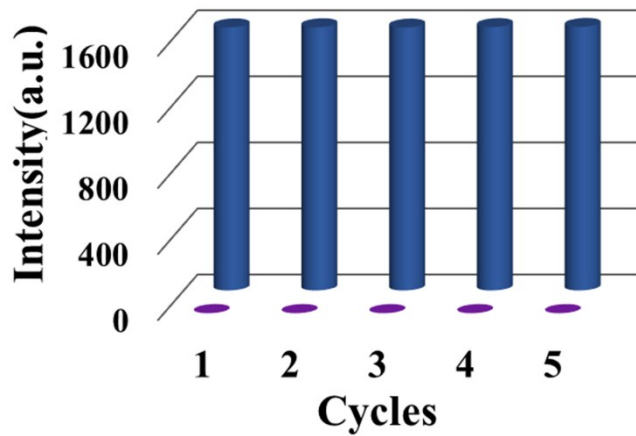


Fig. S8 Photoluminescence intensity of complex **2** in five recyclable experiments for the Fe^{3+} in aqueous solution.

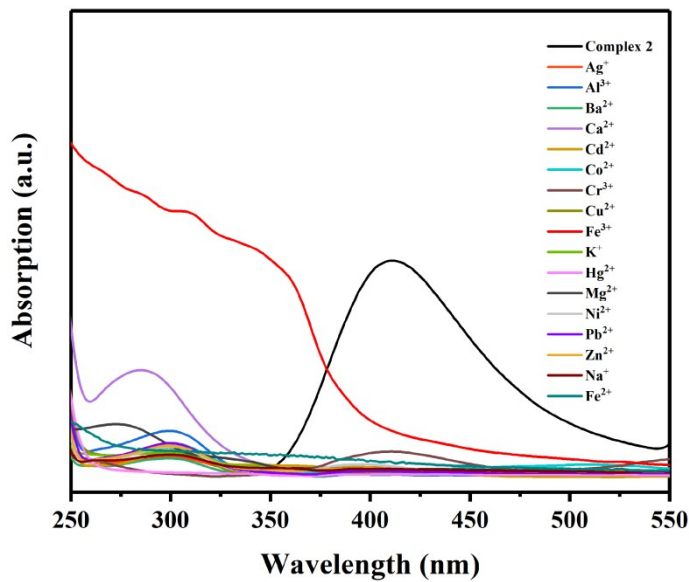


Fig. S9 UV-Vis absorption spectra of various metal cations (0.01 M) aqueous solution. The emission spectra of complex **2** (black color) (2 mg) dispersed in water (2 mL) upon excitation of 280 nm.

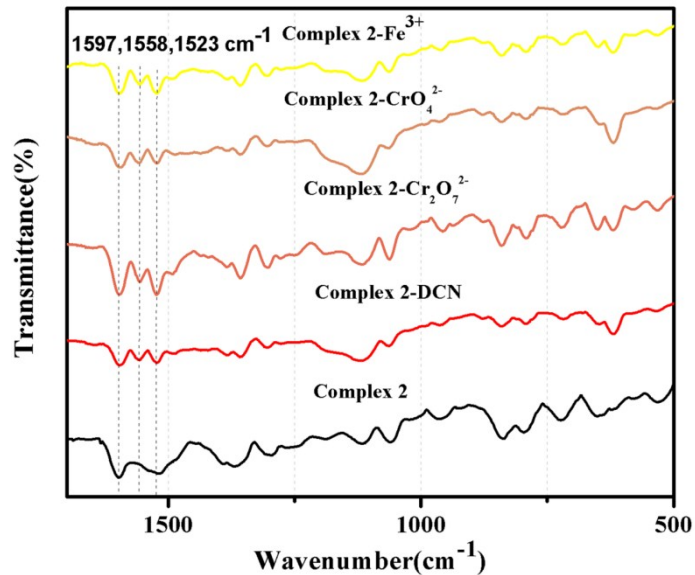


Fig. S10 Changes of part IR for complex **2** before and after the sensing experiments.

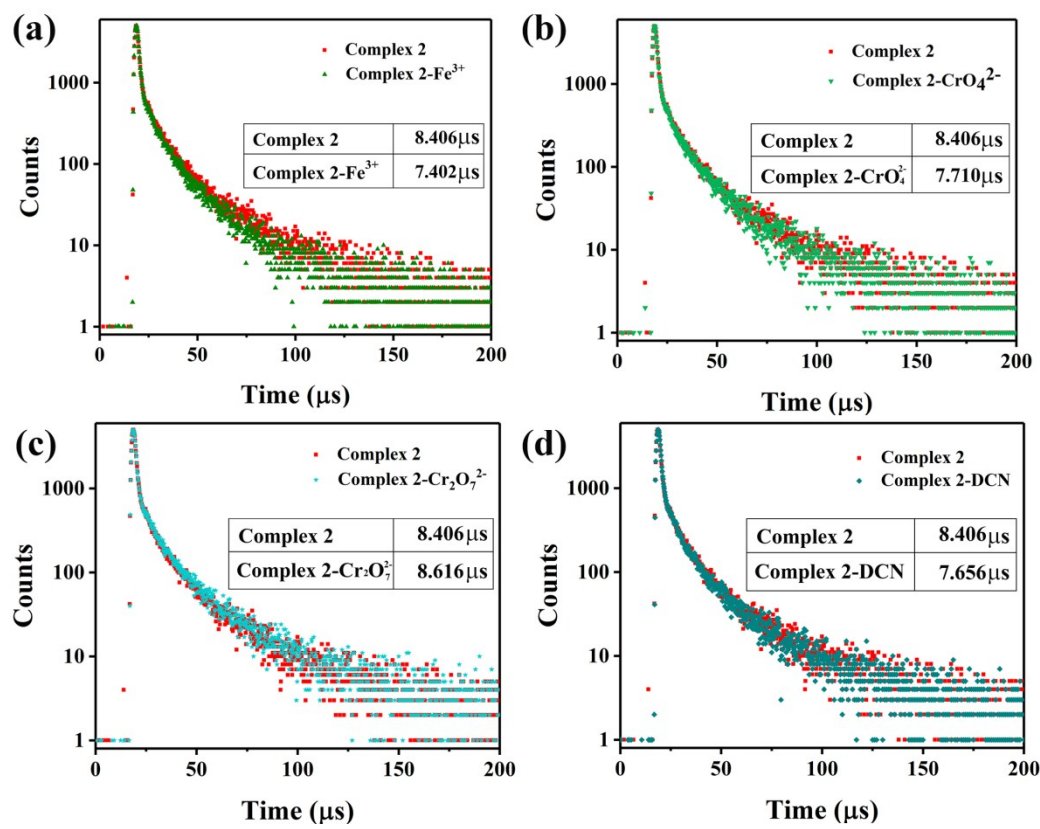


Fig. S11 Lifetime decay profile of complex 2 before and after exposure to Fe^{3+} **(a)**, CrO_4^{2-} **(b)**, $\text{Cr}_2\text{O}_7^{2-}$ **(c)**, DCN**(d)**.

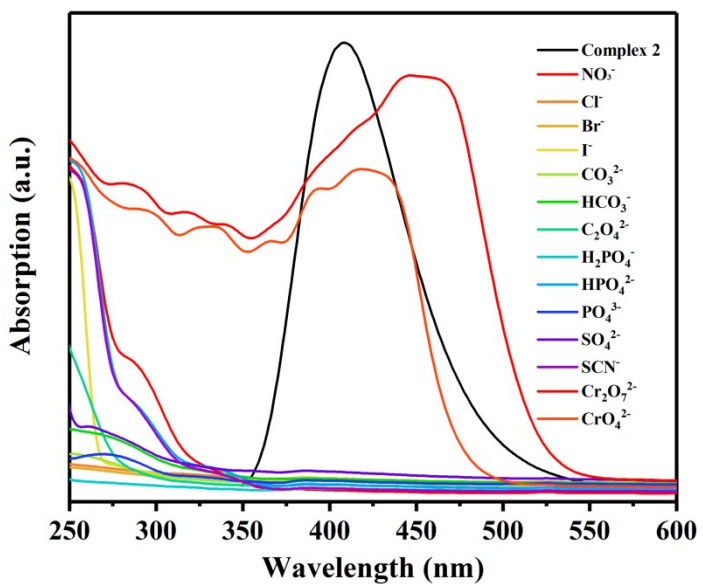


Fig. S12 UV-Vis absorption spectra of various inorganic anions (0.01 M) aqueous solution. The emission spectra of complex **2** (black color) (2 mg) dispersed in aqueous solution (2 mL) upon excitation of 280 nm.

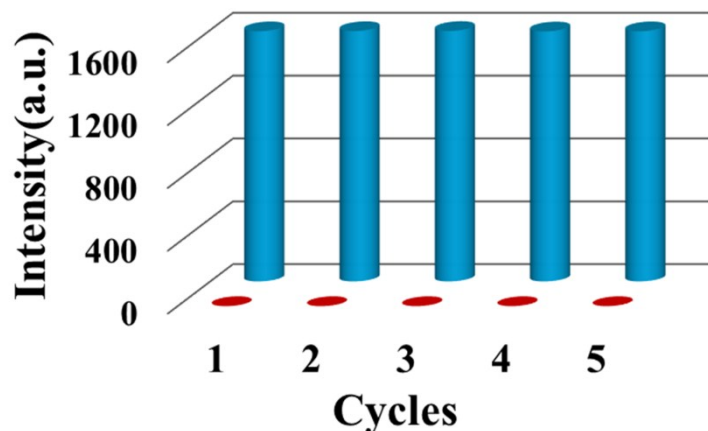


Fig. S13 Photoluminescence intensity of complex **2** in five recyclable experiments for the CrO_4^{2-} in aqueous solution.

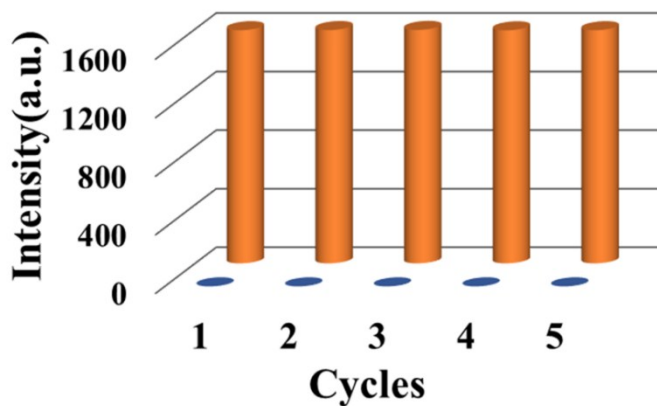


Fig. S14 Photoluminescence intensity of complex **2** in five recyclable experiments for the $\text{Cr}_2\text{O}_7^{2-}$ in aqueous solution.

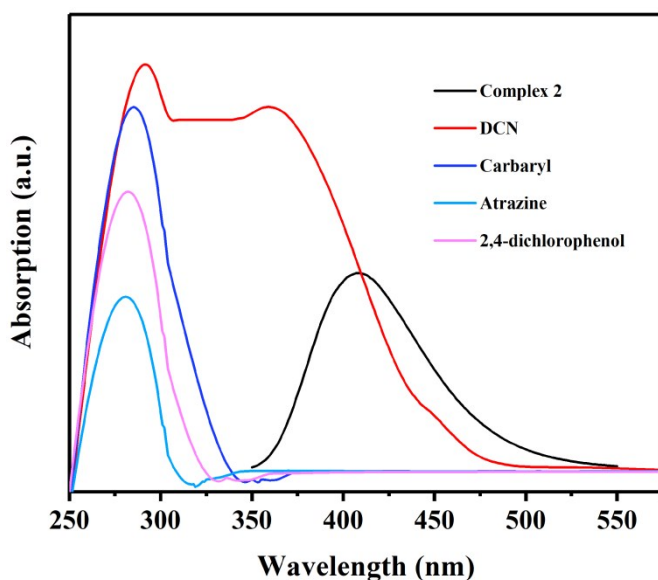


Fig. S15 UV-Vis absorption spectra of various pesticides (0.01 M) DMF solution. The emission spectra of complex **2** (black color) (2 mg) dispersed in DMF (2 mL) upon excitation of 280 nm.

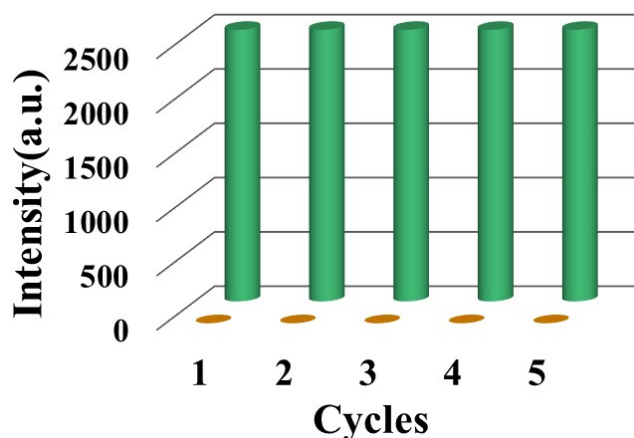


Fig. S16 Photoluminescence intensity of complex **2** in five recyclable experiments for the DCN in DMF solution.